Geophys. J. R. astr. Soc. (1983) **73**, 427–447

Frequency dependence of the quality factor in the upper crust: a deep seismic sounding approach

François Thouvenot *Laboratoire de Géophysique Interne (ERA CNRS No. 603) IRIGM, BP 53 X, 38041 Grenoble, France*

Received 1982 October 20; in original form 1982 September 14

Summary. Ray amplitudes are computed in a one-dimensional velocity structure where the quality factor Q varies continuously with depth. An iterative process is then proposed to derive the quality factor distribution in the upper crust from deep sounding data. Results for compressional waves in the French Massif Central and for a signal frequency close to 20 Hz show that Q increases in a rather linear way from about 40 in surface up to 600 at 7 km depth. Q seems to be higher in the Central Alps: 180 in surface, 1600 at 5 km depth (at 20 Hz). Using proper signal processing, the frequency dependence of Q is finally investigated in the frequency range 10–25 Hz. The results indicate a dependence of the form $Q = Q_0 f^{\alpha}$, where $\alpha = 0.25 \pm 0.1$.

Introduction

Classically wave propagation is considered an adiabatic process, which means that wave motion will continue indefinitely once it has been initiated by some specific source. However, it is common experience that the geometrical spreading factor is only one component of the decrease of wave amplitudes. The other one is commonly known as 'internal friction', even if this term does not seem fortunate (Winkler, Nur & Gladwin 1979), and can be quantified by the so-called quality factor Q. Several excellent review papers have been written recently about the significance of Q measurements and their implications, and the reader is referred to them for a more complete general discussion (Johnston, Toksöz & Timur 1979; Winkler *et al.* 1979).

Although the amount of attenuation is relatively well-known in the mantle on the basis of teleseismic studies, the literature concerning the study of Q in the crust is rather scarce. Up to now only average values have been estimated (e.g. Press 1964), although Clowes & Kanasewich (1970), Berg *et al.* (1971) or Perrier & Ruegg (1973) tried to model the crustal attenuation by a stack of constant-Q layers.

This study has three facets. (1) We first present a new way to model the anelasticity of the upper crust. Q is supposed to increase or decrease continuously with depth while the vertically inhomogeneous velocity model is smoothed with an adequate interpolating curve. Several cases are discussed – interpolation cubic splines, smoothing cubic splines and

exponential splines – which lead to two types of approach – analytical and numerical. (2) A method is then suggested to separate the effects of geometrical spreading and of absorptive losses in seismic signals observed in deep seismic sounding experiments. The method is then successfully tested with a data set previously used by Perrier & Ruegg (1973). (3) We finally show how this method can be used to test the frequency dependence – or constancy – of the quality factor. This problem has turned to a controversy since Rautian & Khalturin (1978) and Aki (1980) ran counter to the constant-Q philosophy professed by Knopoff (1964) and subsequently supported by many authors. This study could thus be viewed as a contribution to the solution of this seismological tangle.

1 Ray integrals and amplitudes with a depth-dependent Q

1.1 THE PROBLEM

We assume that the medium is vertically inhomogeneous, with a coordinate system (x, z) such that the z-axis is perpendicular to the Earth's surface. And we assume that the velocity distribution is specified by a set of velocities v_i at given depths z_i, with $v_{i+1} > v_i$. It is well-known (Chapman 1971; Červený & Pretlová 1977a) that the ray amplitudes are very sensitive not only to interfaces of the first order, but also to interfaces of higher orders. This problem can be solved in several ways.

The analytical approach used by Červený & Pretlová (1977a) is based on a cubic spline interpolation of the velocity/depth distribution, or rather its reciprocal distribution $z = z(v)$. In this case, the cubic spline interpolation is continuous, as well as its first and second derivatives and, moreover, the ray intervals can be evaluated in a closed form.

The numerical approach, first suggested by Chapman (1971), uses basically a cubic spline interpolation $v = v(z)$. Because the velocity/depth distribution is never accurately known, smoothing cubic splines can be used instead, while exponential splines should be reserved for special cases where undesirable oscillations of the cubic spline introduce spurious low-velocity layers.

From the pure mathematical viewpoint, the analytical way looks terse and more attractive. But, because the velocity is the variable of integration, the variation of the quality factor should be expressed as a function of the velocity. Otherwise, one of the ray integrals cannot be evaluated in a closed form and the interest of this method vanishes. By contrast, the numerical method allows a depth dependence of the quality factor and is nevertheless easy to implement. Both approaches are now examined more thoroughly.

1.2 ANALYTICAL APPROACH

We denote the ray parameter by p, and then, if we consider the section of the ray between the depths z_i and z_{i+1}, the corresponding travel time and horizontal distance along this section are the well-known ray integrals

$$t_i = \int_{z_i}^{z_{i+1}} \frac{dz}{v\sqrt{1-p^2v^2}}, \quad x_i = \int_{z_i}^{z_{i+1}} \frac{pv\,dz}{\sqrt{1-p^2v^2}}. \tag{1}$$

If z is expressed as a cubic polynomial in v for any velocity interval $[v_i, v_{i+1}]$

$$z = a_i + b_i v + c_i v^2 + d_i v^3, \tag{2}$$

the ray integrals (1) can be rewritten

$$t_i = b_i I_1^{(i)} + 2c_i I_0^{(i)} + 3d_i I_1^{(i)}, \quad x_i = b_i L_1^{(i)} + 2c_i L_2^{(i)} + 3d_i L_3^{(i)} \tag{3}$$

where

$$I_n^{(i)} = \int_{v_i}^{v_{i+1}} \frac{v^n\, dv}{\sqrt{1-p^2v^2}}$$

and

$$L_n^{(i)} = pI_n^{(i)}. \tag{4}$$

Moreover, the quantity $\partial x_i/\partial p$ which is used in the computation of the geometrical spreading is easy to calculate from equations (3) and (4). We simply obtain:

$$\partial x_i/\partial p = b_i K_1^{(i)} + 2c_i K_2^{(i)} + 3d_i K_3^{(i)} \tag{5}$$

where

$$K_n^{(i)} = \partial L_n^{(i)}/\partial p = \int_{v_i}^{v_{i+1}} v^n (1-p^2v^2)^{-3/2}\, dv. \tag{6}$$

Explicit formulae for $I_n^{(i)}$, $L_n^{(i)}$ and $K_n^{(i)}$ can be found in Červený & Pretlová (1977b).

To introduce attenuation in the model, we need to compute the corresponding absorptive loss factor

$$\exp\left[-\pi f \int_{\text{ray}} (ds/Qv)\right], \tag{7}$$

where f is the frequency of the signal and s the curvilinear abscissa along the ray.

Using the velocity v as the variable of integration, the integral in (7) can be expressed as a sum of quantities t_i^*:

$$t_i^* = \int_{v_i}^{v_{i+1}} \frac{dz}{dv} \frac{dv}{Qv\sqrt{1-p^2v^2}}. \tag{8}$$

It is obvious then that, in order to perform an analytical integration of (8), Q should be a function of v, and not of z.

The first thought would be to suppose a linear dependence of Q with the velocity in each velocity interval $[v_i, v_{i+1}]$

$$Q = B_i(A_i + v). \tag{9}$$

This relationship has a discrepancy of only a few per cent with a linear depth dependence of Q, which is more significant from the physical viewpoint. But, although the closed form evaluation of (8) is possible, it leads to some tedious computations. Therefore, we found it more convenient to use another dependence between Q and the velocity:

$$Q = \frac{A_i}{1+B_i v^2} \tag{10}$$

which, at first, seems sophisticated and unrealistic, but which proves very efficient when introduced in (8):

$$t_i^* = \frac{1}{A_i} \int_{v_i}^{v_{i+1}} \frac{dz}{dv} \frac{dv}{v\sqrt{1-p^2v^2}} + \frac{B_i}{pA_i} \int_{v_i}^{v_{i+1}} \frac{dz}{dv} \frac{pv\, dv}{\sqrt{1-p^2v^2}}. \tag{11}$$

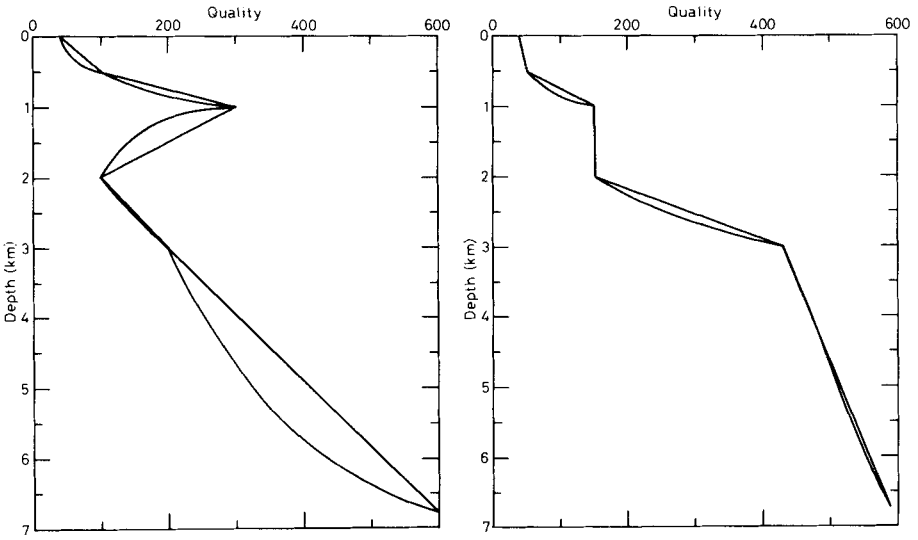

Figure 1. (left) Case of a low quality factor zone sandwiched between two high quality factor zones. (right) Case of a monotonous increase in quality. In both cases, two curves are plotted: (1) the quality factor $Q = A_i/(1 + B_i v^2)$ on each velocity interval $[v_i, v_{i+1}]$, (2) the strictly linear depth dependence of Q on each depth interval $[z_i, z_{i+1}]$. The discrepancy is not very significant, except in the left-hand side case, where the quality factor reversal is responsible for the deviation observed in the depth range 3–7 km. Velocity/depth function given in Table 1.

Clearly, it follows from (1) that

$$t_i^* = \frac{1}{A_i}\left[t_i + \frac{B_i x_i}{p}\right]. \tag{12}$$

In this way, the quantity t_i^* is directly linked to the travel time t_i and to the horizontal distance x_i. It can be seen in Fig. 1 that the relationship given by (10) is usually very close to a strictly linear depth dependence. We put a final stress on the fact that, although this dependence between Q and the velocity does not seem very realistic – Q is most likely more closely related to factors such as fluid content or temperature than it is to velocity – this approach is extremely convenient from the mathematical viewpoint, because the computation of t_i^* is as easy as winking.

Table 1. Velocity/depth distribution in the French Massif Central (Perrier & Ruegg 1973). Depths refer to the altitude of 500 m.

z(km)	v(km s^{-1})
0.000	5.200
0.017	5.211
0.500	5.530
1.000	5.690
2.000	5.840
3.000	5.910
6.800	6.010

1.3 NUMERICAL APPROACH

Using a spline smoothing of the velocity/depth distribution $v = v(z)$ enables a closer contact to be kept with the parameter z. At least three types of spline functions can be used. We will not expatiate on the simple case of strict interpolation splines, but rather consider the case of smoothing splines, first suggested by Červený & Pretlová (1977a). They prove to be advantageous when the velocity/depth distribution involves minute inaccuracies which find expression in crooks and unevenesses when the amplitude/distance curve is computed. Since such inaccuracies are the common share of any velocity/depth determination, usually arrived at with the Wiechert–Herglotz inversion, smoothing splines should be used systematically. At each node z_i, the function $v(z)$ is slightly different from the distribution velocity v_i, but the deviation is usually very small, compared to the error inherent in the determination of v_i. Controlling the extent of smoothing can be achieved by the use of the cross-validation method (see Section 1.4)

The third kind of smoothing which will be finally examined here is the so-called exponential spline smoothing, because it allows us to remove definitely eventual spurious oscillations of the cubic spline. Authors familiar with velocity/depth smoothing are well aware of this problem (Červený & Pretlová 1977a), which is classically solved by introducing additive points in the velocity/depth distribution. Exponential splines constitute an alternative solution. First studied by Späth (1969), they can be viewed as a generalization of cubic splines: in the depth interval $[z_i, z_{z+1}]$, the velocity is expressed by

$$v = a_i + b_i(z - z_i) + c_i \exp\,[\sigma_i(z - z_i)] + d_i \exp\,[-\sigma_i(z - z_i)]. \tag{13}$$

The parameter σ_i controls the tension of the curve on $[z_i, z_{i+1}]$: as σ_i tends to zero, the interpolating curve tends to a cubic spline; for increasing values of σ_i, the curve is more and more straightened, this straightness resulting in a linear interpolation as σ_i tends to ∞.

The velocity/depth distribution being properly interpolated, the non-constancy of Q can now be expressed by

$$Q = A_i + B_i z, \tag{14}$$

and the ray integrals (1) as well as the integral (8) have to be computed numerically. There is no difficulty about this computation, except in the vicinity of the ray turning-point, at depth z_m, where the ray parameter and the velocity are in a reciprocal ratio, and an inverse square-root singularity occurs. It can be shown that these integrals can be reduced, in any case, to

$$I = \int_{z_i}^{z_m} \frac{\phi(z)}{\sqrt{z_m - z}}\, dz \tag{15}$$

where ϕ is a regular function on $[x_i, z_m]$. Changing the variable of integration to

$$\zeta = \frac{z - z_i}{z_m - z_i}, \tag{16}$$

(15) can be written

$$I = \sqrt{z_m - z_i} \int_0^1 \frac{\phi(\zeta)}{\sqrt{1 - \zeta}}\, d\zeta. \tag{17}$$

Using the generalized Gauss quadrature formula, an orthogonal expansion of (17) is

$$I = \sqrt{z_m - z_i} \lim_{n \to \infty} \sum_{k=0}^{n} H_k \phi(\zeta_k) \tag{18}$$

where the coefficients H_k and the points of integration ζ_k are closely connected to the positive roots of the Legendre polynomial of degree $2(n+1)$. Since the convergence of the expansion is very fast, one may safely limit the integration to only half a dozen points.

1.4 COMPUTATION OF THE AMPLITUDE

The alternative closed form approach/numerical approach can be used to compute, for a given ray parameter p, the epicentral distance x, the travel time t and the amplitude at x which can be expressed by the following equation:

$$A(f,x) = A_0(f) \cdot EXG(x) \cdot R(x) \cdot \exp\left[-\pi f \int_{\text{ray}} (ds/Qv)\right], \tag{19}$$

where: $A(f,x)$ is the amplitude spectrum of the recorded arrival; $A_0(f)$ is the source spectrum; $EXG(x)$ is the geometrical spreading factor; and $R(x)$ is the free-surface reflection factor.

Reflection or refraction factors pertaining to waves impinging on velocity discontinuities are not taken into account here, because *we suppose that the velocity increase in the medium is very smooth and that the ray field is regular,* i.e. free of caustics or cusps. This condition is usually met in the real case of a crystalline basement. Another hypothesis which is obvious from equation (19) is that the source line radiates the same amount of energy in any direction. Explosive sources can be considered to have this characteristic in first approximation. We discuss the importance of this assumption later.

2 Application to deep seismic sounding experiments

2.1 DATA

This section describes how deep seismic data can be used to investigate the anelasticity of the upper crust. The data are from experiments which were carried out in 1970 in the western part of the French Massif Central (Fig. 2) on the so-called Millevaches Plateau (Perrier & Ruegg 1973). The Palaeozoic basement outcrops there under the form of muscovite granites. Tectonics and the observation of P_g-waves all agree to consider a vertically inhomogeneous medium a good model of the upper crust in this area. Moreover, no interface is found to occur in the first 10 km of the upper crust.

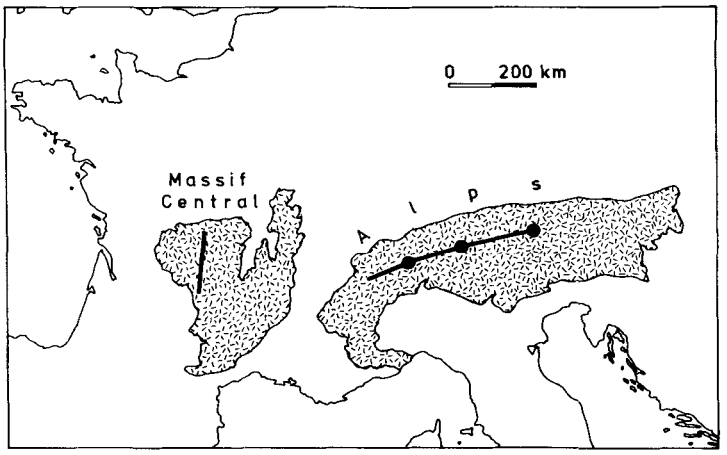

Figure 2. Location of deep seismic profiles used in this study: French Massif Central (Section 2) and Central Alps (Section 3).

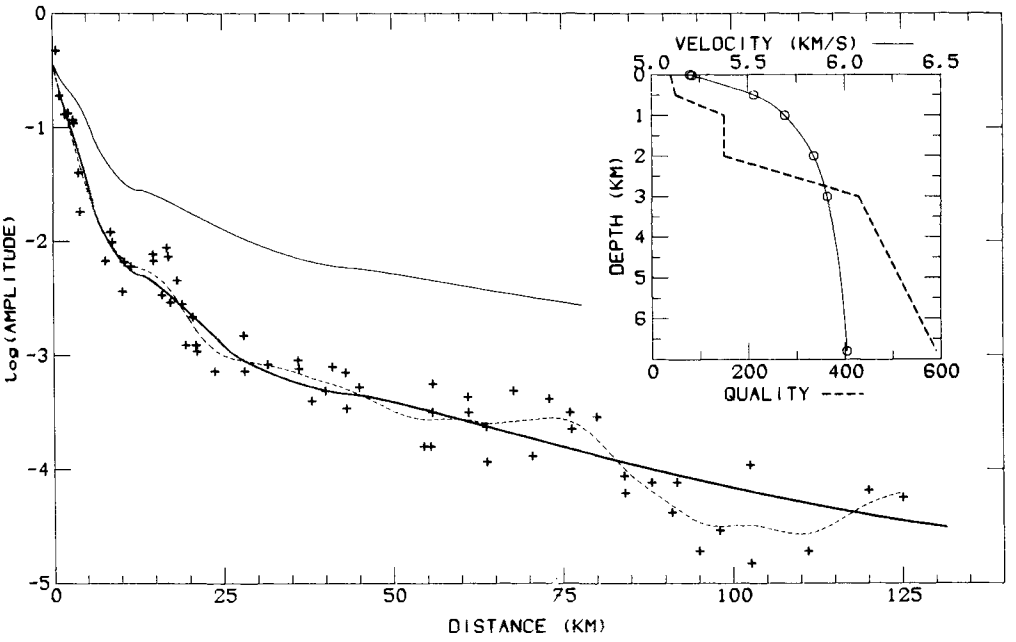

Figure 3. Best fitting Q/depth model for the French Massif Central (heavy dashed line in the box) with the resulting amplitude/distance curve (heavy line). Observed amplitudes (crosses) are smoothed by cross-validation splines (dashed line). The amplitude/distance curve for a perfectly elastic medium is shown for comparison (light line). Same velocity data as in Table 1, now used with an exponential spline interpolation.

The signals were generated by explosive sources and were recorded on analogue tape recorders, which allowed, after digitization, a pliable computer processing. Only vertical component data have been used in this study. Amplitudes of the first arrival were measured on 64 signals with a mean frequency of 18.6 Hz. Distances to shotpoint ranged from 0.5 to 125 km. The velocity model was calculated by Perrier & Ruegg (1973) using the Wiechert–Herglotz inversion.

After correcting the amplitudes for instrument response, they can be plotted on a semi-logarithmic scale (Fig. 3).

2.2 DEFINING THE AMPLITUDE DECREASE

Now comes a perplexing point: what should be the best analytical representation of this data cloud? One would confront the same problem if a line had to be drawn through it by hand. How in particular should the data be smoothed near the shotpoint, where the amplitude decreases rapidly? Should the amplitude measured at the nearest station be taken into account more than others?

Because of its lack of objectivity, a manual smoothing cannot be retained. Turning to smoothing splines does nothing but move the problem back. Denoting indeed by A_i the amplitude measured at the distance x_i, by m the number of data points and restricting for simplicity to the case of cubic splines, the smoothing amounts(?) to seek the solution s_τ of the problem (Reinsch 1967):

$$\underset{f\in H^2[0,x_m]}{\text{minimize}} \left\{\tau \int_0^{x_m} [f''(x)]^2\,dx + \frac{1}{m}\sum_{i=1}^{m} F_i^2(f)\right\} \tag{20}$$

$H_2[0,x_m]$ is the set of real functions defined on $[0,x_m]$ such that f and f' are continuous and the integration of the square of f'' is possible; $F_i(f)$ is an expression involving x_i, A_i and $f(x_i)$.

It remains to choose the smoothing parameter τ, i.e. the balance between the 'smoothness' of s_τ measured by the integral in equation (20) and the 'fidelity' to the data measured by the discrete sum. The cross-validation method (Utreras 1979) allows us to compute this parameter in the following way: if $\sigma_{\tau,k}$ denotes the function solution of the problem

$$\underset{f\in H^2[0,x_m]}{\text{minimize}} \left\{\tau \int_0^{x_m} [f''(x)]^2\,dx + \frac{1}{m}\sum_{\substack{i=1\\ i\neq k}}^{m} F_i^2(f)\right\}, \tag{21}$$

$\sigma_{\tau,k}$ is very similar to s_τ except that the point (x_k, A_k) is not taken into account. Describing the whole data set allows us to build up a set of m functions $\sigma_{\tau,k}$. τ can henceforth be defined as the value minimizing the quantity

$$V(\tau) = \frac{1}{m}\sum_{k=1}^{m} [A_k - \sigma_{\tau,k}(x_k)]^2. \tag{22}$$

Routines developed by Utreras (1979), which are very time-efficient even for many data points, have been used to compute τ and thus obtain an unbiased analytical representation of the amplitude decrease.

2.3 INVERSION PROCESS

The Q distribution is described by a set of n nodes (z_i, Q_i) and linear – or pseudo-linear – interpolations between them. At the beginning of the process, the Q/depth function is supposed *a priori* to be constant throughout the crust. In the case under study we used a constant value of 300. But this trial value has no influence on the final Q/depth model.

An iterative process is applied at each node in order to fit the analytical representation of the amplitude decrease. For a given Q/depth function, the extent of fitting is defined by the standard deviation of amplitudes calculated for rays having their turning-points at depths $\{z_i\}$ $(i = 2,\ldots,n)$. Each Q_i is adjusted until the best fitting is obtained.

Once it has been performed on the deepest node, the process is iterated, but now the amplitude standard deviation is calculated for rays having their turning-points at depths.

$$\{z_{i-1} + (z_i - z_{i-1})/2, z_i\} \qquad (i = 2,\ldots,n).$$

At iteration number k, the ray set is defined by the series

$$\{z_{i-1} + (z_i - z_{i-1})/k, z_{i-1} + 2(z_i - z_{i-1})/k, \ldots, z_i\} \qquad (i = 2,\ldots,n).$$

Thus, the model is quickly roughed out, the solution being sharpened only in the further iterations (Fig. 4). A couple of iterations is generally sufficient to stabilize the Q/depth function (Thouvenot 1981). For a typical data set of about 100 observed amplitude points and for a velocity/depth distribution of 10 nodes or so, the computing time is 1 min on an HB68 system.

2.4 RESULTS

The resulting amplitude/distance curve (heavy line in Fig. 3) can be compared to the amplitude/distance curve for a perfectly elastic medium. The difference between the two

Figure 4. Convergence of the Q models towards the final solution. Two different representations are displayed: (a) Q/depth plot for 10 iterations of the inversion process, the size of the symbols being in relation with the order of iteration and the final solution being shown in heavy line; (b) convergence of the quality factor at a given depth versus the order of iteration. Six iterations are usually sufficient to stabilize all values.

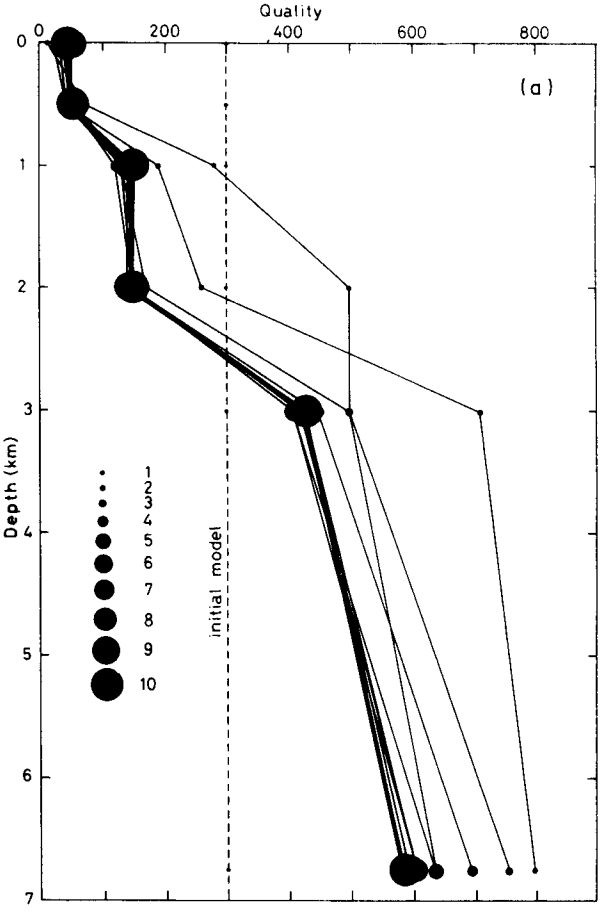

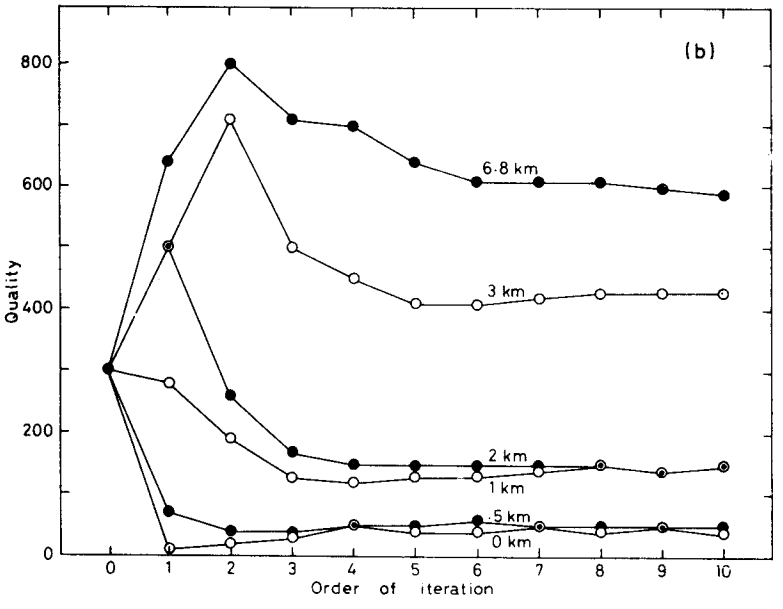

curves at large distances is more than one logarithmic unit and reflects the influence of absorptive losses in the upper crust. Q increases in a rather linear way from about 40 in surface up to 600 at 7 km depth.

This Q/depth function is somewhat different from results by Perrier & Ruegg (1973). Basically, this is due to the fact that these authors kept up a linear interpolation between the nodes of the velocity/depth distribution. The velocity gradient and its first derivative were then discontinuous. Consequently, their Q values (300 at most) are lower than ours. But maybe the most interesting difference stands in the trend of Q at large depths. Results by Perrier & Ruegg (1973) show a kind of stabilization of the quality factor around the value of 300. And this effect can be felt even at the moderate depth of 3 km. Our results do not imply any stabilization of the sort: the quality factor still increases at depth and high Q values of about 1000 would thus characterize the middle crust.

3 Testing the frequency dependence of Q

Testing the frequency dependence of the quality factor in the upper crust is the very first idea coming to the mind when the inversion process is fully understood. If one is able to define the observed amplitude decrease for a given frequency, a proper frequency analysis of the seismic signals should provide a series of Q/depth models. Finally, the evolution of the quality factor at a given depth as a function of frequency should give valuable information on the frequency trend.

Data used in this section were collected along the 1975 Alpine Longitudinal Profile (ALP 75) in South Switzerland and Western Austria (Fig. 2). This part of the profile runs across the Penninic Domain (Bernhard and Silvretta Nappes), the Aar-Gotthard crystalline complex and the Austro-Alpine Domain (Oetztal Nappes) with a short cut through the Engadin window (Alpine Explosion Seismology Group 1976). Three shotpoints are used in this study, with two shots in each place. All of them are situated in the crystalline basement: gneissic complex of the Gotthard Massif for the western shotpoint; upper Austro-Alpine

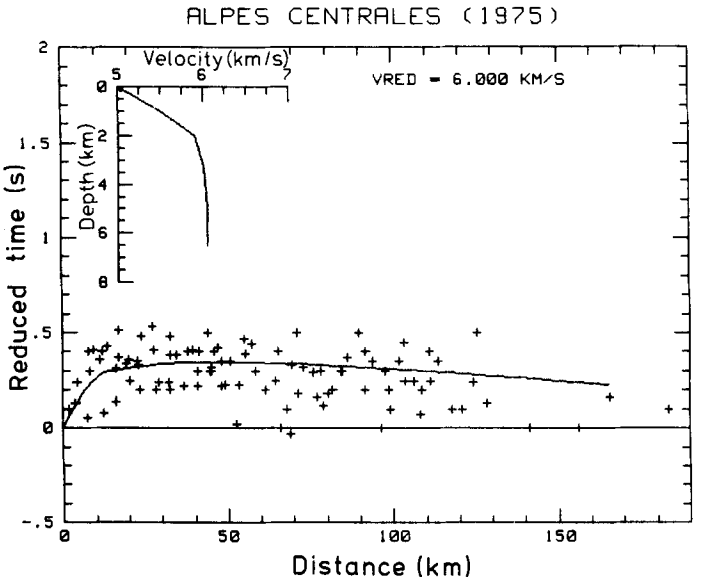

Figure 5. Observed reduced travel times for the central part of the ALP 75 profile and velocity/depth structure (Central Alps).

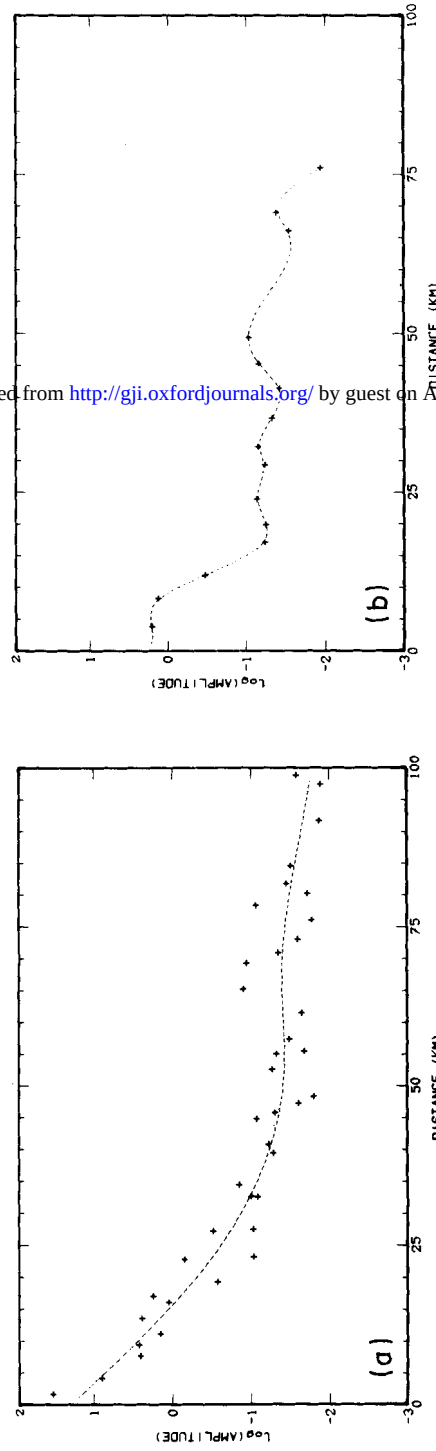

Figure 6. How a composite decrease of observed amplitudes is built. (a, b, c) Observed amplitudes for three different shotpoints on three different sections of the ALP 75 profile; respectively: western shotpoint recorded to the east and to the west, middle shotpoint recorded to the west and eastern short point recorded to the west; data are scaled for shot weight and smoothed by cross-validation splines. (d) Composite decrease of observed amplitudes; allowance has been made for differences in the efficiency of the shots.

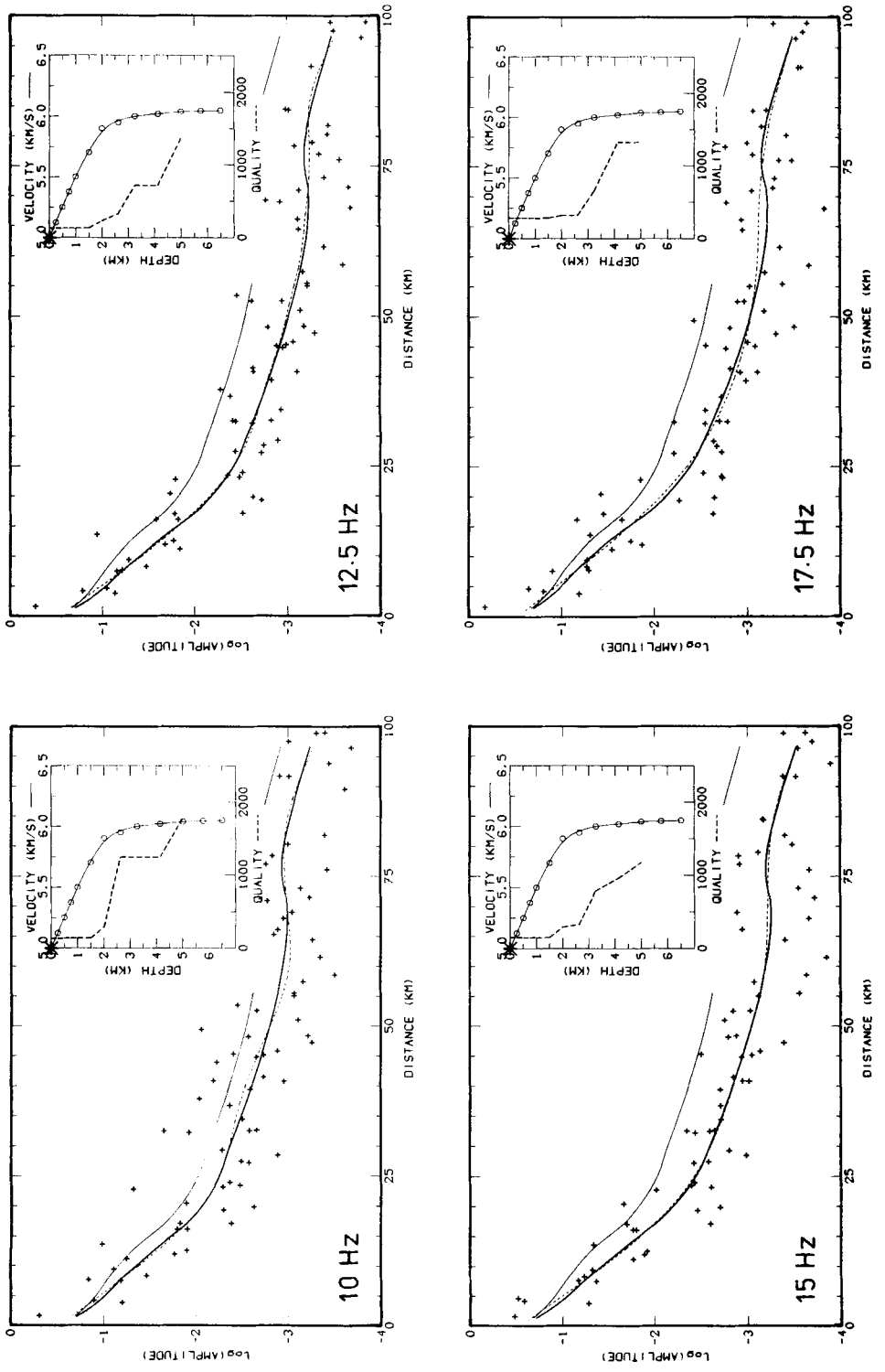

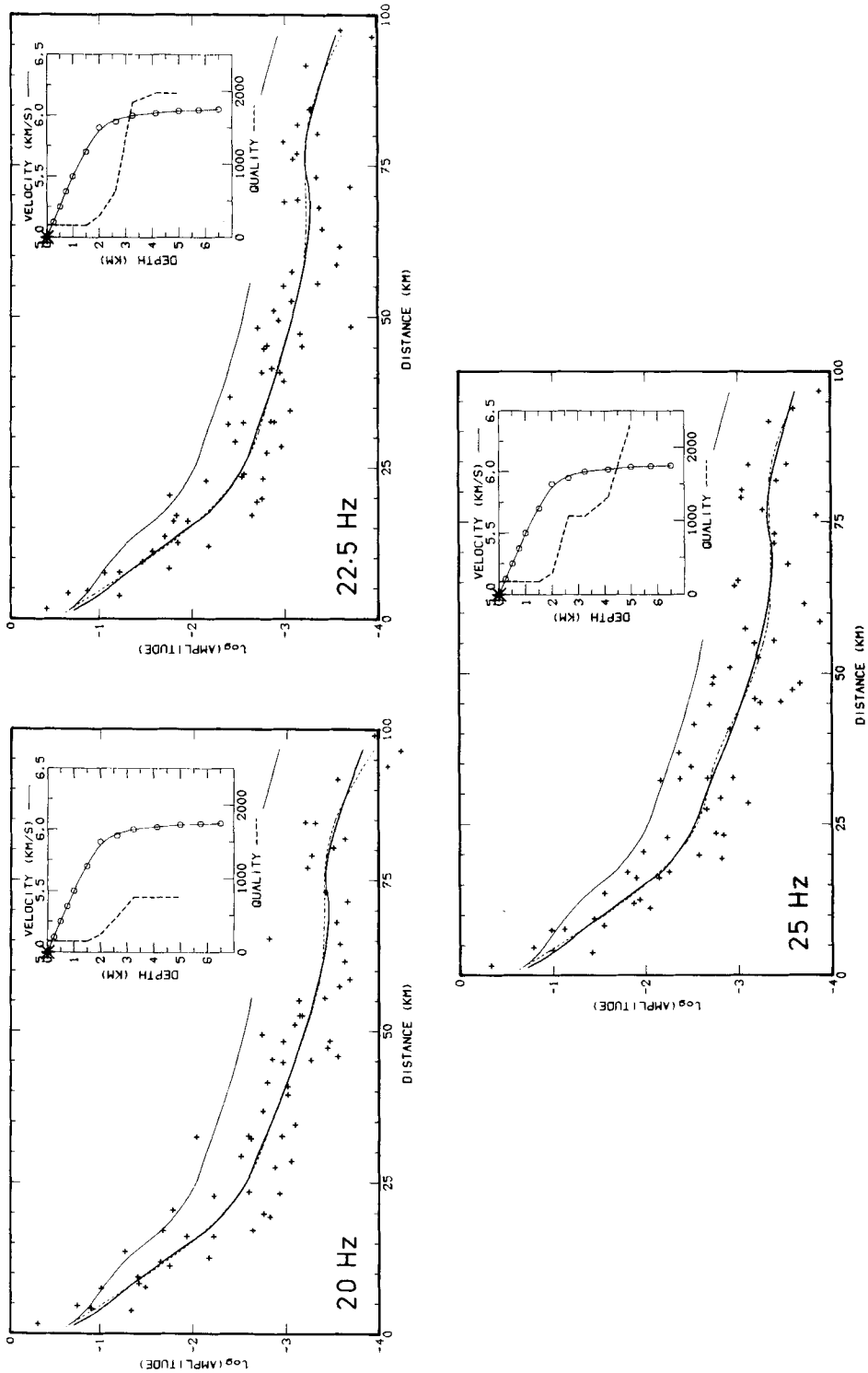

Figure 7. *Q* models for the Central Alps as a function of frequency. For each frequency, the *Q*/depth model displayed is the one which provides the best fit of observed amplitude data. Refer to Fig. 3 for a further description.

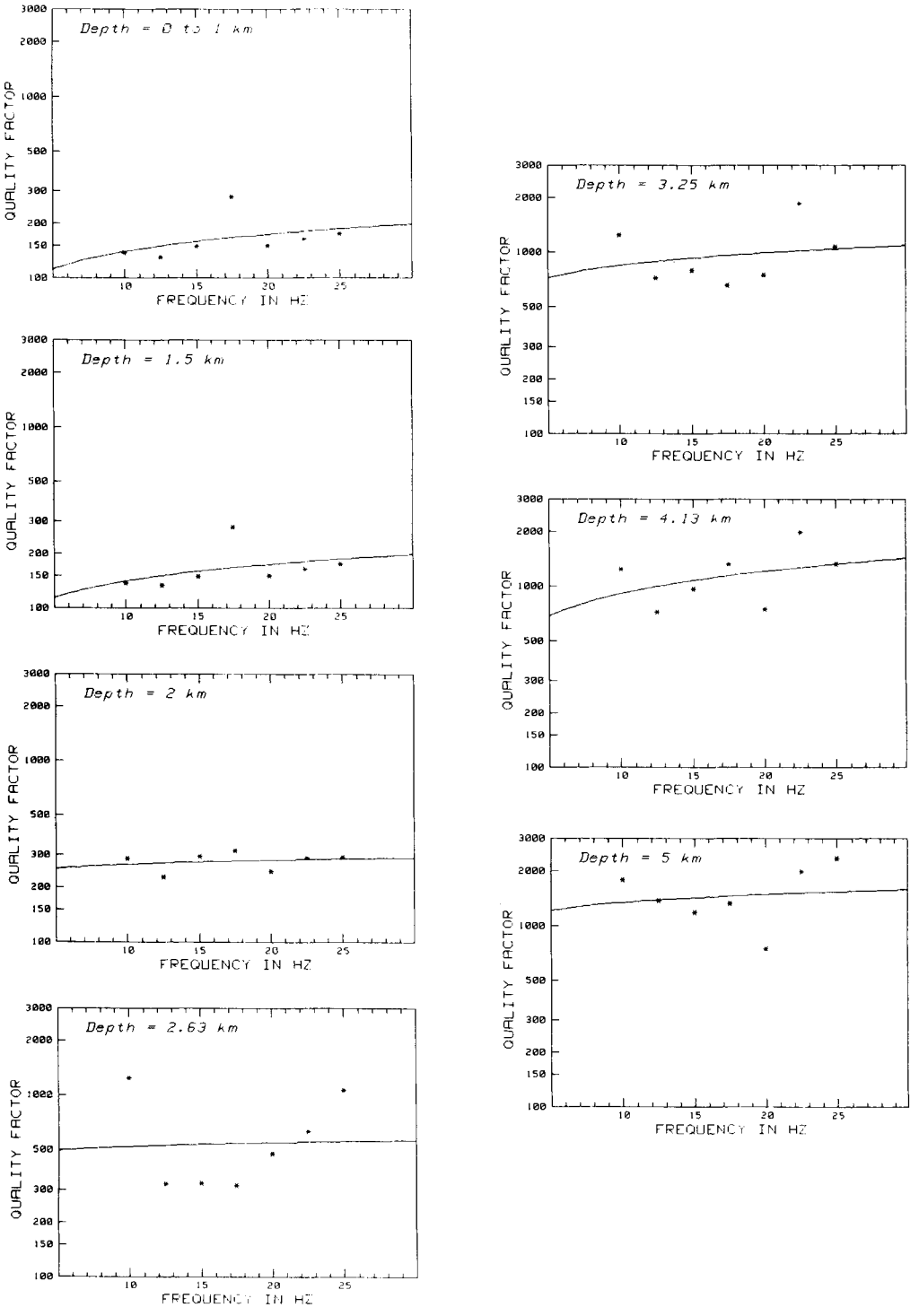

Figure 8. Frequency dependence of Q in the upper crust (Central Alps). For each depth, Q values arrived at by the inversion process are analysed using a logarithmic regression $Q = Q_0 f^{\alpha}$. Depths refer to the altitude of 1000 m.

basement for the middle shotpoint; lower Austro-Alpine nappe (Innsbrücker Quarzphyllit) for the eastern shotpoint. A detailed analysis of P_g-waves in each section of ALP 75 (Ottinger 1976; Miller, Gebrande & Schmedes 1977) shows no evidence of strong interfaces in the velocity models of the upper crust. Observed travel times are plotted as a composite section in order to get a synthetic velocity/depth function (Fig. 5 and Table 2).

The next step is to perform several bandpass filterings of the data. The following values were retained: 8–12; 10–15; 12–18; 14–21; 16–24; 18–27 and 20–30 Hz. For each filtering, the amplitude of the first arrival is measured, when possible, in each station not beyond 100 km. It seems actually far more sensible to limit amplitude measurements to signals where the first arrival is clear rather than to measure without rhyme or reason. Up to 100 km, the signal:noise ratio is mostly adequate and the data density is approximately constant – one point every 1.5 km or so – whether in the vicinity of the shotpoint or in the range 90–100 km.

To take the shot weight into account, amplitudes are scaled by $W^{2/3}$, where W is the weight of explosives in tons. Amplitude data for each shot are first smoothed separately using the cross-validation method (Fig. 6) and then put together after a proper adjustment has been performed to balance the efficiency of the shots. The cross-validation method is applied once more to obtain a composite analytical decrease of observed amplitudes for the frequency under study. This analytical decrease is ultimately used as the starting point of the Q inversion process.

Q models arrived at are shown in Fig. 7, together with the relevant amplitude curves. Values are rather consistent in the very upper crust – down to 1.5 km depth – but are more scattered further below (Table 2). This is due to the fact that Q values at depth are drastically sensitive to the near-horizontality of amplitude curves in the range 60–100 km. This scattering reflects the limit of the method and values in Table 2 are significant up to only two digits at most.

The frequency dependence can nevertheless be analysed at each depth (Fig. 8). A logarithmic regression $Q = Q_0 f^{\alpha}$ is applied and the values of α and Q_0 are given in Table 2.

Table 2. Velocity and quality factor distribution as a function of depth and frequency in the Central Alps. Depths refer to the altitude of 1000 m. A logarithmic regression $Q = Q_0 f^{\alpha}$ is performed at each depth and the values of α and Q_0 are given together with the standard deviation. The mean value of α is 0.25 ± 0.1.

			frequency (Hz)								
z(km)	v(km/s)	Q_0	10	12.5	15	17.5	20	22.5	25	α	St.Dev.
0.000	5.000	67	137	130	149	278	150	164	175	0.317	0.064
0.250	5.125	"	"	"	"	"	"	"	"	"	"
0.500	5.250	"	"	"	"	"	"	"	"	"	"
0.750	5.375	"	"	"	"	"	"	"	"	"	"
1.000	5.500	"	"	"	"	"	"	"	"	"	"
1.500	5.700	69	137	133	149	278	150	164	175	0.307	0.063
2.000	5.900	222	287	228	294	317	244	291	292	0.079	0.016
2.625	5.950	439	1242	325	326	317	477	633	1062	0.073	0.397
3.250	6.000	496	1242	717	787	657	748	1850	1062	0.229	0.160
4.125	6.020	354	1242	717	959	1323	748	1974	1322	0.409	0.133
5.000	6.040	954	1784	1370	1175	1323	748	1974	2345	0.147	0.170
5.750	6.045										
6.500	6.050										

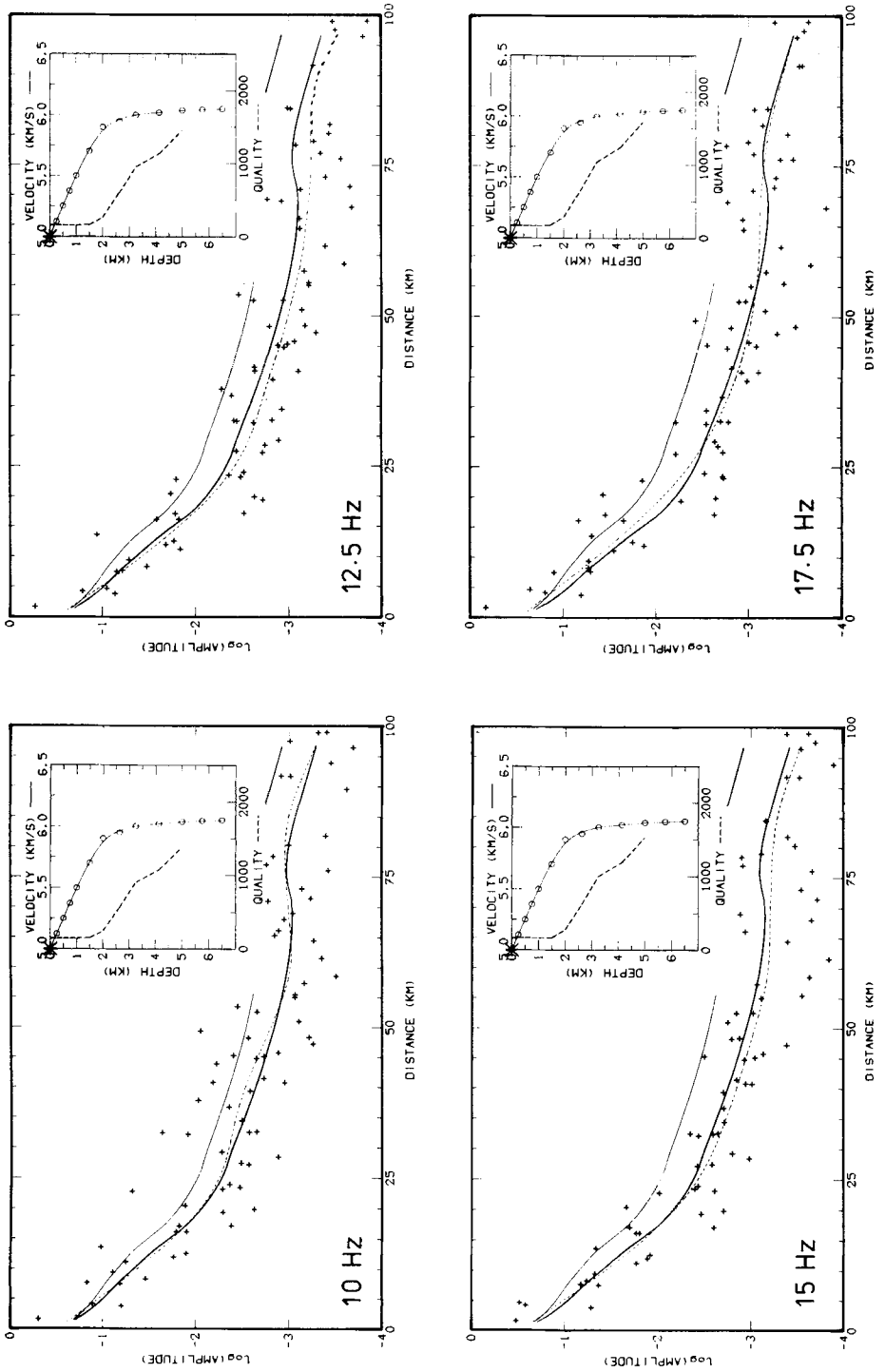

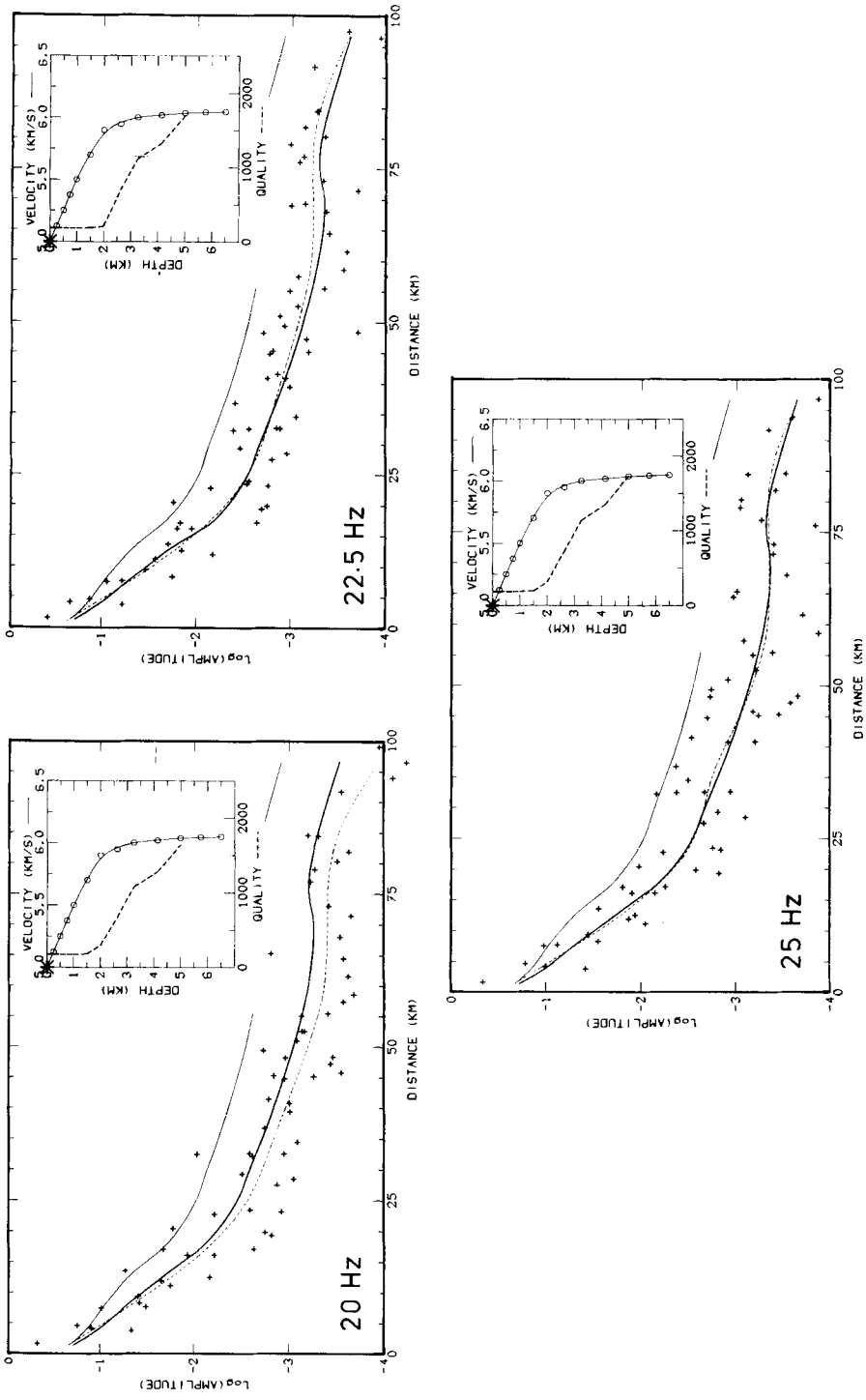

Figure 9. Smoothed Q models of the Central Alps as a function of frequency. Q models used here are slightly different from the raw models resulting from the inversion process and shown in Fig. 7: they take the frequency dependence into account. However, there is no excessive misfit between the observed amplitude curve (dashed line) and the computed amplitude curve (heavy line). The consistency of Q in the first 1.5 km is followed by a quasi-linear increase in the depth range 1.5–5 km.

Table 3. Final quality factor distribution in the Central Alps. Assuming that $\alpha = 0.25$, Q values given in Table 2 are smoothed by $Q_0 f^{0.25}$. Q_0 values in column 2 represent the quality factor tendency for a frequency of 1 Hz.

		frequency (Hz)						
z(km)	Q_0	10	12.5	15	17.5	20	22.5	25
0.000 to 1.000	83	148	157	164	171	176	182	186
1.500	84	149	157	164	171	177	182	187
2.000	137	244	258	270	280	290	298	306
2.625	306	545	576	603	626	648	667	685
3.250	498	886	937	981	1019	1054	1085	1114
4.125	586	1043	1103	1154	1199	1240	1277	1311
5.000	756	1344	1421	1487	1546	1598	1646	1690

Although some fits are disputable because of a high standard deviation, e.g. at 2.63 km depth, a plain dependence is evidenced where $\alpha = 0.25 \pm 0.1$. Adopting this value for α, Q values given in Table 2 can be smoothed and a synthetic Q/depth function can be built which takes into account Q values at all depths and at all frequencies (Table 3). Fig. 9 shows the extent of misfit introduced when amplitude curves are again calculated using this synthetic Q/depth function. The misfit is usually hardly perceptible, which shows how difficult it is to decide between a value of 1000 or 2000 at depth. What definitely appears is the constancy of Q in the first 1.5 km, followed by a quasi-linear increase in the depth range 1.5–5 km.

4 Discussion

We have already emphasized how difficult it is to get accurate estimations of Q. In the present method, this lack of precision can be ascribed mainly to the horizontal trend of amplitude curves at large distances. We do not think, however, that Q values arrived at using other methods are more reliable: most of them are even rougher because they do not take the geometrical spreading properly into account. Three more factors can be set forth to explain the relative inaccuracy of the present method: (1) scarcity of amplitude observations; (2) invalidity of the smooth one-dimensional velocity model; and (3) assumption of an isotropic radiation of the source.

Amplitude measurements should be very numerous in the vicinity of the shotpoint, where the amplitude decreases rapidly with distance. The slope of the observed curve in the first few kilometres of the profile has a drastic influence on the estimation of Q in surface. For instance, it would not be surprising that high Q values found in the surface in the Central Alps are only related to the relative lack of information in the first 5 km of the profile: only four data points are usually available (Fig. 9), whereas, for the Massif Central inversion, observations are twice as numerous in the same distance range (Fig. 3). At large distances there is a further need to multiply amplitude measurements in order to free oneself from station effects which scatter the observations. However, for the data sets used in this study, this condition is sensibly met.

As for the second factor pointed out above – validity or invalidity of the smooth one-dimensional velocity model – it would, of course, be preposterous to pretend that no strong interfaces occur in the upper crust, in the French Massif Central as well as in the Central Alps. The profiles used in this study stretch over several geological units, even though the

one on the Millevaches Plateau is of a rather superior quality because of the homogeneity of the granitic basement. Even in this case, we are not secure from reflections produced by discrete layering in intrusives for instance. However, a careful examination of the signals shows a clear lack of strong interfaces which could be traced with reliability. Thus we are in a position to claim that, if large velocity changes exist, they are purely local and contribute to the dispersion of the data points in what we called 'station effects'.

When we computed amplitudes (Section 1.4), we assumed the radiation of the source to be isotropic, i.e. any elementary ray tube departing from the shotpoint contains the same elementary amount of energy. This assumption is most likely invalid if the explosion is in sediments, because refraction into the basement will modify the radiation pattern. Shots used in this study were all fired in the crystalline basement and should therefore escape this criticism. Still we are fully aware that geological conditions near the shotpoints are of the utmost importance and potential shotpoints for such Q studies should be selected consequently.

As a partial conclusion, it can be noted that *Q values given in this paper should be considered significant up to only two digits at most.* For instance, it would not be sound to try a comparison between two values of Q such as 1500 and 1200. However, when we state that Q in the French Massif Central is 600 at 7 km depth whereas it is 1600 in the Central Alps at a comparable depth, the difference is tangible and should reflect, in our view, a physical reality.

As was pointed out in the introduction, much ink has been spilt over the frequency dependence of the quality factor since the early 1960s, when this mechano-electrical analogy was first introduced in seismology. The controversy has been confined for a long time mainly to theoretical discussions and, although some ultrasonic experiments have been carried out in the past two decades, too few field studies are available at present.

Table 4 is a synopsis of studies of the frequency dependence of Q in the crust. All of them, except this study, used natural earthquakes as sources and most of them are relative to the quality factor for shear waves (Q_S) or coda waves (Q_c). If the physical significance of Q_S can be easily understood, some questions may arise about Q_c. This quantity cannot be introduced as Q_P was in equation (7), but rather looked at as a characterization of the turbidity of the lithosphere. Although Aki (1980) undoubtedly associated Q_c with Q_S, we do not feel inclined to follow this equivalence. Because we do not as yet know how strongly scattering

Table 4. Frequency dependence of the quality factor in the crust.

location	depth investigated	$Q^{(*)}$	frequency range (Hz)	Q values	sources	frequency dependence	authors
California	upper crust	Q_S	2 - 10	75 - 100	quakes	constant Q	Bakun & Bufe (1975)
U.S.S.R.	lithosphere	Q_c	0.05 - 15	30 - 3000	quakes	$\propto f^{0.5}$	Rautian & Khalturin (1978)
Pyrenees (France)	crust	Q_c	3 - 24	40 - 2300	quakes	$\propto f^{1.2}$	Hinderer (1979)
Japan	lithosphere	Q_S	0.05 - 25	150 - 1000	quakes	$\propto f^{0.6} - f^{0.8}$	Aki (1980)
North Eastern America	lithosphere	Q_S	0.025 - 1	150 - 2000	quakes	$\propto f^{0.7} - f^{0.5}$	Mitchell (1980)
Western Europe	lithosphere	Q_p	1 - 10	100 - 1000	quakes	$\propto f^{0.8} - f^{0.9}$	Rouchon et al. (1981)
Hindu Kush	lithosphere	Q_c	0.4 - 48	30 - 2000	quakes	$\propto f^{0.5} - f^{1.0}$	Roecker et al. (1982)
California	upper crust	Q_S	3 - 25	60 - 500	quakes	$\propto f^{1.0}$	Singh et al. (1982)
Central Alps	upper crust	Q_p	10 - 25	180 - 1600	explosions	$\propto f^{0.25}$	this study

(*) Q_p = Q for compressional waves ; Q_s = Q for shear waves ; Q_c = Q for coda waves $\sim Q_S$, after Aki (1980)

affects any portion of any particular wave, we do not pretend that *P*-waves are unaffected by scattering. But we stress that Q for coda waves, because is quantifies mainly scattering effects, is of a different nature than for compressional or shear waves.

This study is thus the first to approach the frequency dependence of Q_P using explosions as seismic sources – hence the difficulty in comparing numerical results. The exponent of frequency, $\alpha = 0.25$, is lower than in most studies, although values found by Mitchell (1980) are somewhat similar. As opposed to the poor precision which characterizes Q values, this estimation of α is reliable, because of the use of the same velocity/depth function throughout the frequency range investigated. It is particularly obvious that data presented in Fig. 8 *cannot* be fitted by f^{α}-curves where $\alpha = 0.5$–1.0. These values have nevertheless been widely used previously in spectral studies of source parameters.

5 Conclusions

(1) The inversion process allows us to derive the quality factor distribution in the upper crust from deep seismic sounding data under the following assumptions:

(i) the velocity structure is one-dimensional (no lateral variations);

(ii) the velocity/depth function is known with accuracy;

(iii) this function is continuous (no interface of the first order) and increases monotonously with depth (regularity of the ray field in the Červený's sense);

(iv) amplitude measurements – hence recording stations – are very numerous, especially in the vicinity of the shotpoint, where the amplitude decreases rapidly with distance; a spacing of 500 m should be typically used between the stations.

These conditions are usually met in the case of a crystalline basement with no – or not much – sedimentary cover, provided that the area has been properly surveyed by several profiles.

(2) For the French Massif Central and for a frequency of about 20 Hz, Q_P increases in a rather linear way from 40 in surface up to 600 at 7 km depth. For the Central Alps, and for the same frequency, somewhat higher values of Q_P are found: 180 in surface, 1600 at 5 km depth. Although Q values are difficult to estimate with accuracy, especially at depth, this difference is not believed to be due to a computing artifice and should reflect a physical reality.

(3) The middle crust seems to be characterized by high Q values (1000–2000).

(4) In the frequency range 10–25 Hz, the frequency dependence of the quality factor is $Q = Q_0 f^{\alpha}$, where $\alpha = 0.25 \pm 0.1$. This value is much lower than in previous studies. The discrepancy could be explained by the fact that previous determinations of α wave tainted with scattering effects, while ours is not.

Acknowledgments

I am indebted to V. Červený for stimulating suggestions when this work was still in progress. G. Perrier was the initiator of this study and his help is gratefully acknowledged. The French participation to the ALP 75 experiment was financed by Institut National d'Astronomie et de Géophysique under INAG grant ATP 32-46.

References

Aki, K., 1980. Attenuation of shear waves in the lithosphere for frequencies from 0.05 to 25 Hz, *Phys. Earth planet. Int.*, **21**, 50–60.

Alpine Explosion Seismology Group, 1976. A lithospheric seismic profile along the axis of the Alps, 1975. I: First results, *Pageoph,* **114,** 1109–1130.

Bakun, W. H. & Bufe, C. G., 1975. Shear-wave attenuation along the San Andreas fault zone in Central California, *Bull. seism. Soc. Am.,* **65,** 439–459.

Berg, J. W. (Jr), Long, L. T., Sarmah, S. H. & Trembly, L. D., 1971. Crustal and mantle inhomogeneities as defined by attenuation of short-period *P* waves, in *The Structure and Physical Properties of the Earth's Crust,* ed. Heacock, J. G., *Monogr. Am. geophys. Un.,* **14,** 51–57.

Bouchon, M., Massinon, B., Mechler, P. & Nicolas, M., 1981. *Attenuation of Local Phases in Western Europe,* Advanced Research Projects Agency and European Office Aerospace Research and Development, 27 pp.

Červený, V. & Pretlová V., 1977a. Application of smoothed splines in the computation of ray amplitudes of seismic body waves, *Publ. Inst. Geoph. Pol. Acad. Sci.,* **115,** 187–197.

Červený, V. & Pretlová, V., 1977b. Computation of ray amplitudes of seismic body waves in vertically inhomogeneous media, *Studia geophys. geod.,* **21,** 249–255.

Chapman, C. H., 1971. On the computation of seismic ray travel times and amplitudes, *Bull. seism. Soc. Am.,* **61,** 1267–1274.

Clowes, R. M. & Kanasewich, E. R., 1970. Seismic attenuation and the nature of reflecting horizons within the crust, *J. geophys. Res.,* **75,** 6693–6705.

Hinderer, J., 1979. Etude du facteur de qualité *Q* de la région Arette-Larrau (Pyrénées Atlantiques) à partir de la coda des séismes locaux, *Dipl. Eng. Geoph.,* University of Strasbourg, 70 pp.

Johnston, D. H., Toksöz, M. N. & Timur, A., 1979. Attenuation of seismic waves in dry and saturated rocks: II. Mechanisms, *Geophysics,* **44,** 691–711.

Knopoff, L., 1964. *Q, Rev. Geophys. Space Phys.,* **2,** 625–660.

Miller, H., Gebrande, H. & Schmedes, E., 1977. Ein verbessertes Strukturmodell für die Ostalpen, abgeleitet aus refraktions-seismischen Daten unter Berücksichtigung des Alpen-Längsprofils, *Geol. Rdsch.,* **66,** 289–308.

Mitchell, B. J., 1980. Frequency dependence of shear wave internal friction in the continental crust of Eastern North America, *J. geophys. Res.,* **85,** 5212–5218.

Ottinger, T., 1976. Der Aufbau der Erdkruste unter dem schweizerischen Teil des Refraktionsseismischen Alpen-Längsprofils von 1975, *Dipl. Eng.,* Federal Institute of Technology, Zurich, 170 pp.

Perrier, G. & Ruegg, J. C., 1973. La structure profonde du Massif Central français, *Ann. Géophys.,* **29,** 435–502.

Press, F., 1964. Seismic wave attenuation in the crust, *J. geophys. Res.,* **69,** 4417–4418.

Rautian, T. G. & Khalturin, V. I., 1978. The use of the coda for determination of the earthquake source spectrum, *Bull. seism. Soc. Am.,* **68,** 923–948.

Reinsch, C., 1967. Smoothing by spline functions, *Num. Math.,* **10,** 177–183.

Roecker, S. W., Tucker, B., King, J. & Hatzfeld, D., 1982. Estimates of *Q* in Central Asia as a function of frequency and depth using the coda of locally recorded earthquakes, *Bull. seism. Soc. Am.,* **72,** 129–150.

Singh, K., Fried, J., Apsel, R. & Brune, J., 1982. Spectral attenuation of *SH*-wave along the Imperial Fault and a preliminary model of *Q* in the region, *Bull. seism. Soc. Am.,* in press.

Späth, H., 1969. Exponential spline interpolation, *Computing,* **4,** 225–253.

Thouvenot, F., 1981. Modélisation bi-dimensionnelle de la croûte terrestre en vitesse et atténuation des ondes sismiques. Implications géodynamiques pour les Alpes Occidentales, *thesis,* University of Grenoble, 211 pp.

Utreras, F., 1979. Utilisation de la méthode de validation croisée pour le lissage par fonctions splines à une ou deux variables, *thesis,* University of Grenoble, 192 pp.

Winkler, K., Nur, A. & Gladwin, M., 1979. Friction and seismic attenuation in rocks, *Nature,* **277,** 528–531.